IJE TRANSACTIONS A: Basics Vol. 33, No. 10, (October 2020) 1968-1977

International Journal of Engineering

Journal Homepage: www.ije.ir

A Proposed Approach for Separation between Short Circuit Fault, Magnetic Saturation Phenomenon and Supply Unbalance in Permanent Magnet Synchronous Motor

Z. Gherabi*[a], D. Toumi[b], N. Benouzza[a], A. Bendiabdellah[a]

[a] *Electrical Engineering Faculty, Diagnosis Group, LDEE Laboratory, University of Sciences and Technology of Oran (USTO-MB), Algeria*
[b] *Electrical Engineering Department, L2GEGI Laboratory, University of Ibn-Khaldoun of Tiaret, Algeria*

PAPER INFO

Paper history:
Received 31 October 2019
Received in revised form 12 July 2020
Accepted 21 July 2020

Keywords:
Fault Indicators
Inter-Turns Short-Circuit Fault
Magnetic Saturation Phenomenon
Permanent Magnet Synchronous Motor
Supply Voltage Unbalance

ABSTRACT

This paper proposes a new approach for discrimination between short circuit fault, magnetic saturation phenomenon and supply voltage unbalance in permanent magnet synchronous motor. This proposed approach is based on tracking the simultaneous position in the polar coordinates of the amplitude and phase angle of the voltage and current indicator FFT signals of the harmonics characterizing the three phenomena. The voltage indicator set using three supply voltages to check the status of the power source. In the same way, the current indicator defined using three line currents to discriminate between the short circuit fault and the magnetic saturation phenomenon. To highlight the effectiveness and the capability of this approach, a series of simulations are performed on signals obtained from a permanent magnet synchronous motor mathematical model. This model is based on a 2D-extension of the modified winding function approach.

***doi**: 10.5829/ije.2020.33.10a.15*

NOMENCLATURE

PMSM	: Permanent Magnet Synchronous Motor	UVU	: Under-Voltage Unbalance
ITSC	: Inter-Turns Short-Circuit	OVU	: Over-Voltage Unbalance
MSP	: Magnetic Saturation Phenomenon	FFT	: Fast Fourier Transform
SVU	: Supply Voltage Unbalance	ANN	: Artificial Neural Network

1. INTRODUCTION

The main industrial application areas, related to electric traction, processing, machining, material shaping, and recently electric propulsion are increasingly implementing the PMSM. These have a more compact structure, a high mass power, a higher dynamic response compared to conventional structures [1–4].

Although these motors are reliable, under certain electrical, thermal, mechanical, or environmental constraints, they are subjected to unexpected failures. Among these failures, approximately 30 % to 40 % fall into the category of faults related to stator windings [5–7]. For this reason, early detection of this type of fault is important because a simple ITSC can produce more severe damage. This detection will preserve the safety of goods and people and avoid the unscheduled shutdown of the production line and therefore increases the life of these motors and minimize financial losses.

Several diagnostic techniques have been developed to detect this type of fault, depending on the selected physical quantities [8–16]. Among these techniques, the spectral analysis of the stator current is a promising approach. Its main advantages are the easy installation of the sensors and the information richness of the current spectrum for the detection of almost all faults that can appear in the electrical machines. Indeed, several studies [8, 9] have shown that the ITSC fault is manifested by the increase of the third harmonic amplitude of the PMSM current spectrum.

*Corresponding Author Email: *zgherabi@yahoo.com* (Z. Gherabi)

Please cite this article as: Z. Gherabi, D. Toumi, N. Benouzza, A. Bendiabdellah, A Proposed Approach for Separation between Short Circuit Fault, Magnetic Saturation Phenomenon and Supply Unbalance in Permanent Magnet Synchronous Motor, International Journal of Engineering (IJE), IJE TRANSACTIONS A: Basics Vol. 33, No. 10, (October 2020) 1968-1977

Unfortunately, these signatures may also be due to the SVU and the MSP. The appearance of these three phenomena by the creation of the same harmonics makes it difficult to discriminate between them.

Several techniques have been recently deployed to discriminate between the ITSC faults from other secondary phenomena such as MSP and SVU [17–19].

Paper [17] presents a simple method for the diagnosis and the discrimination between the ITSC fault and the SVU. The authors of this paper have used the ANN approach, where they chose the percentage of the amplitude of the third harmonic compared to the fundamental one, as input quantities in different cases of the motor operation. Unfortunately, the method used does not deal with the distinction of the third harmonic due to the MSP. In [18], a structure using a feed-forward type ANN, based on the analysis of active and reactive power to discriminate between a stator ITSC fault and an SVU in induction motors, is proposed. The simulation and experimental results obtained show the advantage of the use of the phase shift between the two powers as a simple diagnostic technique compared to the analysis of the signals of the stator current. Despite the advantages presented by these two techniques, they have significant drawbacks, such as the absence of a systematic method to define the best topology of the neural network and the number of neurons in the hidden layer.

To overcome the various drawbacks mentioned above, this paper proposes a new approach of separation between the ITSC fault, the MSP, and the SVU in PMSM. This approach is based on tracking the simultaneous position in the polar coordinates of the amplitude and phase angle of the FFT signals of the voltage and the current indicator of the harmonic characterizing of three phenomena. The voltage indicator set using the three supply voltages to check the status of the power source. In the same way, the current indicator defined using three line currents to discriminate between the ITSC fault and the MSP. To highlight the effectiveness of this approach, a series of simulations will be carried out on a known and improved PMSM model. This model is based on the modified winding function approach, of which the permanent magnet is considered as a fictitious coil traversed by an excitation current $''\, i_f\, ''$.

2. INTER-TURNS SHORT-CIRCUIT

Electrical faults such as the degradation of the insulating material are internal faults that develop in the machine during its operation. They are caused by the increased temperature of the winding and stator yoke, natural thermal aging of the material, mechanical stresses at start-up, lack of eccentricity, contamination caused by hydrocarbons and moisture, and the fast switching of power electronics components [20, 21]. In most cases, this degradation causes an ITSC fault, which can generate a very large value of the current flowing in the short-circuit branch of the phase, which results in excessive heating of the conductors. In its operating conditions, a failure can be caused after a few minutes of its start. In fact, and as a rule, an increase of 10 °C in temperature compared to its nominal value, reduces the life of drivers twice as fast [22]. On the other hand, the ITSC fault also causes a risk of the permanent magnets irreversible demagnetization and the saturation of the magnetic circuit due to the high magnetic field.

3. MAGNETIC SATURARATION PHENOMENON

The saturation of ferromagnetic materials is a complex physical phenomenon that is difficult to model. In electrical machines, the MSP first appears in areas where the cross-section of the magnetic field lines is the weakest, usually in the stator and rotor teeth, but also in polar arcs for machines with salient poles; therefore, it is a local phenomenon. One of the leading causes of magnetic saturation is the increase of the current, which consequently causes an increase in the intensity of the magnetic field. Therefore, the magnetic induction is beyond the saturation bend. This increase in current is caused either by an increase in the supply voltage or by an ITSC fault [23–25]. To detect the MSP, a problem arises because many studies have proven that the MSP indicators manifest themselves in the same signatures as those of the ITSC fault [23–25].

4. UNBALANCE OF POWER SUPPLY VOLTAGE

A three-phase system is said to be unbalanced or asymmetrical if the three-phase voltages and currents do not have the same amplitude and/or are not out of phase with each other by 120 °. This phenomenon is one of the most common interferences in electrical systems. The unbalances are generally due to single-phase loads because, in this case, the currents absorbed on the three phases are of amplitude and/or different phases, resulting in an unbalance of the three voltages. Voltage unbalance can also be due to three-phase loads, when these are not symmetrical. Indeed, several cases of SVU have the same unbalance factor but have different effects on the loads. Among these unbalances, one can quote [26–28]:

- Under-voltage: decrease of a single-phase, two phases, or all three phases at the same time.
- Over-voltage: increase of a single-phase, two phases, or all three phases at the same time.

To diagnose this type of phenomenon by the stator current spectral analysis technique. Several studies [26–28] have shown that the SVU is manifested with the same signatures as those of the ITSC fault and the MSP.

The appearance of the effect of these three phenomena on harmonics of the same frequency makes the distinction between them a difficult task.

The purpose of our work is to develop a new approach to discriminate between these three phenomena. To do this, it is crucial to establish a mathematical model of the Permanent Magnet Synchronous Motor.

5. MODELING OF THE HEALTHY PMSM

The modeling approach is based on a semi-analytical method of Permanent Magnet Synchronous Motor. This modeling method is rather generic in the sense that it relies on a description of the electromagnetic couplings within the machine based on the geometric and constitutive topology of the machine. This approach has already been proven for the modeling of squirrel cage induction machines [29, 30]. It has also been adapted to the PMSM in [31, 32]. In this section, we will present more precisely the model where the taking into account of permanent magnets is carried out, to preserve the notion of magnetic coupling with the stator, by the use of the fictitious coils.

5. 1. Modeling of Permanent Magnets The modeling method is based on the exploitation of an Ampere model which makes it possible to identify a permanent magnet whose magnetization M to the distribution of fictitious currents (ampere currents) constituted by:

- A surface current density σ defined by:

$$\vec{\sigma} = \vec{M} \wedge \vec{ds} \tag{1}$$

- A surface volume current density ρ defined by:

$$\vec{\rho} = rot(\vec{M}) \tag{2}$$

In our case, the permanent magnet is characterized by a constant magnetization. Thanks to the Equations (1) and (2) of the ampere model, we can deduce that there exists a fictitious surface current density. In contrast, the volume current density is zero because of the constant magnetization. In conclusion, we can represent the permanent magnet of the rotor by fictitious coils traversed by currents, as illustrated in Figure 1, which will allow us to implement the magnetically coupled electrical circuit approach [32].

5. 2. Modeling of the Machine The PMSM equation system can be represented as fellow [21, 32]:

$$\begin{bmatrix} V_{sa} \\ V_{sb} \\ V_{sc} \end{bmatrix} = \begin{bmatrix} R_s & 0 & 0 \\ 0 & R_s & 0 \\ 0 & 0 & R_s \end{bmatrix} \begin{bmatrix} i_{sa} \\ i_{sb} \\ i_{sc} \end{bmatrix} + \frac{d}{dt} \begin{bmatrix} \phi_{ia} \\ \phi_{ib} \\ \phi_{ic} \end{bmatrix} + \frac{d}{dt} \begin{bmatrix} \phi_{ma} \\ \phi_{mb} \\ \phi_{mc} \end{bmatrix} \tag{3}$$

Such that:

$[V_{sabc}] = [V_{sa} \quad V_{sb} \quad V_{sc}]^T$: Stator voltages vectors;

$[i_{sabc}] = [i_{sa} \quad i_{sb} \quad i_{sc}]^T$: Stator currents vectors;

$[R] = R_s[I]$: Stator résistance matric;

$[\phi_i] = [\phi_{ia} \quad \phi_{ib} \quad \phi_{ic}]^T$: Stator fluxes vectors;

$[\phi_m] = [\phi_{ma} \quad \phi_{mb} \quad \phi_{mc}]^T$: Mutual fluxes vectors between stator and rotor.

where,

$$\begin{bmatrix} \phi_{ia} \\ \phi_{ib} \\ \phi_{ic} \end{bmatrix} = \begin{bmatrix} L_{aa} & M_{ab} & M_{ac} \\ M_{ba} & L_{bb} & M_{bc} \\ M_{ca} & M_{cb} & L_{cc} \end{bmatrix} \begin{bmatrix} i_{sa} \\ i_{sb} \\ i_{sc} \end{bmatrix} \tag{4}$$

The mutual fluxes between the stator and the rotor of a machine consisting of 4 poles (corresponding to 4 fictitious coils) are given by the following matrix system [21, 32]:

$$\begin{bmatrix} \phi_{ma} \\ \phi_{mb} \\ \phi_{mc} \end{bmatrix} = \begin{bmatrix} M_{saf1} & M_{saf2} & M_{saf3} & M_{saf4} \\ M_{sbf1} & M_{sbf2} & M_{sbf3} & M_{sbf4} \\ M_{scf1} & M_{scf2} & M_{scf3} & M_{scf4} \end{bmatrix} \begin{bmatrix} i_{f1} \\ i_{f2} \\ i_{f3} \\ i_{f4} \end{bmatrix} \tag{5}$$

The modeling of the rotating part of the machine is based on the use of Newton's second law. We will have:

$$J\frac{d}{dt}\Omega + F\Omega = C_{em} - C_r \tag{6}$$

By carrying out an energy balance, it is shown that the electromagnetic torque is equal to the partial derivative of the magnetic Co-energy with respect to the position of the rotor. Consequently, the torque is expressed by the following equation [21, 32]:

$$C_{em} = \frac{\partial W_{comag}}{\partial \theta_r} = [i_{sabc}]\frac{\partial [M_{ss}]}{\partial \theta_r}[i_{sabc}] + [i_{sabc}]\frac{\partial [M_f]}{\partial \theta_r}[i_f] \tag{7}$$

6. INDUCTANCES CALCULATION

It is essential to know that the accuracy of inductance calculation is the crucial point for a successful PMSM

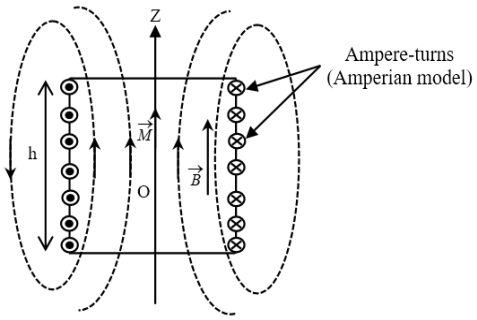

Figure 1. Illustration of the ampere model on a cylindrical permanent magnet [19]

simulation. All inductances are calculated by using the winding function approach [29–31], which is based on the following formula:

$$L_{A.B} = \mu_o rl \int_o^{2\pi} N_A(\varphi,\theta_r) n_B(\varphi,\theta_r) g^{-1}(\varphi,\theta_r) d\varphi \quad (8)$$

where, μ_o is the air permeability, r is the mean radius of the gap, l is the actual length of the machine, $N_A(\varphi,\theta_r)$ is the winding function of the winding '' a '', $n_B(\varphi,\theta_r)$ is the distribution function of the winding '' b '' and $g^{-1}(\varphi,\theta_r)$ is the inverse of the gap function (see Figure 2).

6. 1. Inductances Calculation in the Healthy Case

To calculate the PMSM inductances in the healthy case, the air gap becomes uniform, so the inverse of the air gap $g^{-1}(\varphi, \theta_r)$ must be constant and equal to the inverse of the nominal air gap g_o, which therefore allows the Equation (8) to be rewritten as follows:

$$L_{ab} = \frac{\mu_o rl}{g_o} \int_o^{2\pi} N_a(\varphi,\theta_r) n_b(\varphi,\theta_r) d\varphi \quad (9)$$

6. 2. Inductances Calculation in the Presence of MSP

The MSP can be modeled by a variation in the function of the air gap [24, 25].

The inductances calculation is made in the same way as in the one of a uniform air gap, except the inverse of the air gap function is replaced by the following equation:

$$g(\varphi,\theta_r) = g_o\left[1 - k_{gsat}\, cos(\,2(p\varphi - \theta_f))\right] \quad (10)$$

$$g^{-1}(\varphi,\theta_r) = \frac{1}{g_o}\left[1 + k_{gsat}\, cos(\,2(p\varphi - \theta_f))\right] \quad (11)$$

where g_o is the average value of the gap length, φ is the position of the stator, θ_f is the position of the air gap flux, p is the pole pair number, $kgsat$ is the saturation factor.

6. 3. Inductances Calculation in the Presence of ITSC Fault

The presence of the fault modifies the equation system of the PMSM, so when the Short circuit occurs between the turns of the phase '' a '', the system of the Equation (3) becomes [21, 22]:

$$\begin{bmatrix} V_{sa} \\ V_{sb} \\ V_{sc} \\ V_{sd} \end{bmatrix} = \begin{bmatrix} R'_{sa} & 0 & 0 & 0 \\ 0 & R_{sb} & 0 & 0 \\ 0 & 0 & R_{sc} & 0 \\ 0 & 0 & 0 & R_{sd} \end{bmatrix} \begin{bmatrix} i_{sa} \\ i_{sb} \\ i_{sc} \\ i_{sd} \end{bmatrix} + \frac{d}{dt} \begin{bmatrix} \phi_{ia} \\ \phi_{ib} \\ \phi_{ic} \\ \phi_{id} \end{bmatrix} + \frac{d}{dt} \begin{bmatrix} \phi_{ma} \\ \phi_{mb} \\ \phi_{mc} \\ \phi_{md} \end{bmatrix} \quad (12)$$

The inductances calculation is made in the same way as in the healthy PMSM. During an ITSC, the winding function of the faulty phase '' a '' changes as well as its inductance, its resistance, and its mutual inductances with the other branches of the PMSM [21].

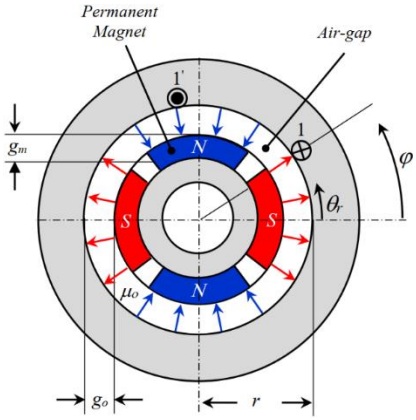

Figure 2. Cross-section of 4 poles surface-mounted PMSM with main dimensions

7. PROPOSED APPROACH

The approach proposed in this paper aims to precisely discriminate between the effects of ITSC failures to those due to secondary phenomena such as the SVU and the MSP. The flowchart (Figure 4) of the proposed method is briefly explained by the procedure steps below:

1st Step: Generation of the signature of the current and the voltage from the simulated model

2nd Step: Determination of the voltage indicator

- Extraction of the voltage indicator by the use of the following equation:

$$ind\_v(t) = |V_{sa} - V_{sb}| + |V_{sb} - V_{sc}| + |V_{sc} - V_{sa}| \quad (13)$$

- Calculation of the spectra (amplitude and phase angle) of this indicator by using the FFT.
- Determination from the spectra of the voltage indicator the magnitude and phase angle of the harmonic characteristics of the power unbalance that is (2fs).

$$\begin{cases} mag = |ind\_v(f)|_{f=2f_s} \\ \varphi = arg(ind\_v(f))_{f=2f_s} \end{cases} \quad (14)$$

With: $ind\_v(f) = FFT(ind\_v(t))$

- Plot of the position in polar coordinates as a function of the magnitude and the phase angle of the harmonic (2fs), as shown in Figure 3.

3rd Step: Determination of the current indicator

- Extraction of the current indicator by the use of the following equation:

$$ind\_i(t) = |I_{sa} - I_{sb}| + |I_{sb} - I_{sc}| + |I_{sc} - I_{sa}| \quad (15)$$

- Calculation of the spectra (amplitude and phase angle) of this indicator by using the FFT.
- Determination from the current indicator spectra of the amplitude and the phase angle of the ITSC fault and the MSP characteristic harmonic.
- Plot of the position in polar coordinates as a function of the amplitude and phase angle of the harmonic (2fs) as shown in Figure 3.

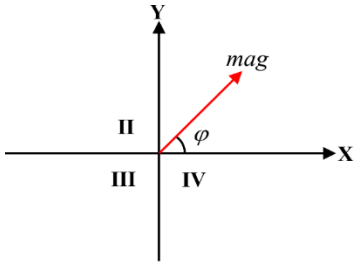

Figure 3. Representation in polar coordinates of the amplitude and phase of the second harmonic ($2f_s$)

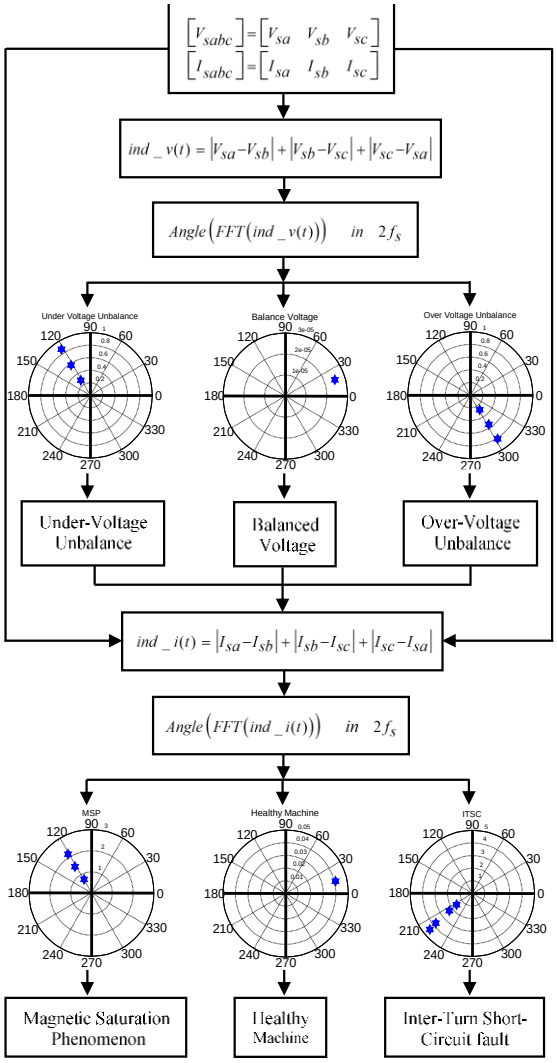

Figure 4. Flowchart of the proposed approach

4th Step: Exploitation of the voltage and current indicator in the separation between the ITSC fault and the secondary phenomena

First, the state of the power source is determined by tracking the position of the plot (in one of the four quadrants) of the voltage indicator.

- If the plot position is in the first quadrant, this implies the absence of power unbalances.
- The presence of under-voltage or over-voltage unbalances indicated by the position of the voltage indicator plot in the second and fourth quadrants, respectively.

Secondly, the ITSC fault is discriminated from the MSP fault by tracking the position of the plot (in one of the four quadrants) of the current indicator.

If the plot position is in the first quadrant, this implies the absence of the ITSC fault and the MSP.

- If the plot is positioned in the second quadrant, this implies the existence of the MSP. However, if it is placed in the third quadrant, this means the presence of the ITSC fault.

It is necessary to note that the SVU does not influence the current indicator. In the same way, the presence of the MSP or the ITSC faults does not influence the voltage indicator.

8. SIMULATION RESULTS

To demonstrate the effectiveness of the proposed approach, a mathematical model of the PMSM developed in Section 5 is used for the different modes of operation:

- Healthy PMSM powered by a balanced voltage;
- Healthy PMSM powered by unbalanced voltage;
- Motor operation in the presence of the ITSC fault;
- Motor operation in the presence of the MSP.

The simulation is performed on a PMSM with the following specifications: 3.6 kW, 4 poles, 36 stator slots, and 4 fictitious rotor coils. The arrangement of the stator and the rotor windings of this motor and its parameters are indicated in the appendix (Table A). The mathematical model obtained, and all the expressions of the inductances are implemented under the MATLAB environment. In all the simulations of this work, the machine at no-load is started, and a load torque is applied at the instant 0.5 s. The load torque corresponds to that of the nominal torque of 17.5 Nm.

8. 1. Analysis of the Current by the Classical Power Spectral Density Estimation

The spectral analysis of the obtained stator currents signature from the mathematical model of the simulated PMSM gives us the following results according to the established operating mode.

8. 1. 1. Healthy PMSM Powered by Balanced Voltage

Figure 5 illustrates the stator current spectrum in the healthy motor operation mode (without ITSC fault, without MSP, and with a balanced power source).

It can be noted that the spectrum contains in addition to the fundamental harmonic, a series of harmonics that

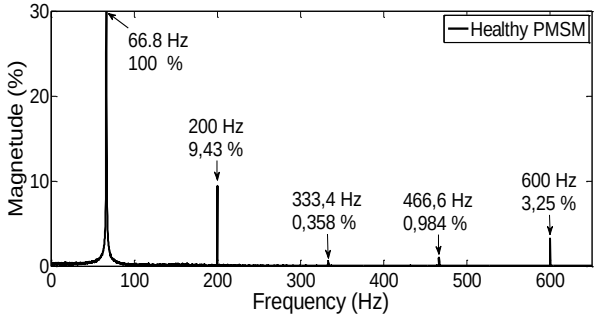

Figure 5. Healthy PMSM powered by a balanced voltage: Stator current spectrum

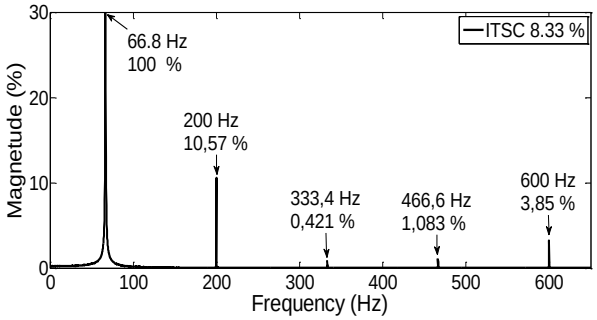

Figure 7. Motor operation in case of 8.33 % ITSC fault: Stator current spectrum

represents the space harmonics whose frequencies can easily be checked using the Equation (16). This spectrum will be considered as the reference one.

$$f_{sh} = [2.k + 1]f_s \quad (16)$$

8. 1. 2. Healthy PMSM Powered by Unbalanced Voltage Figure 6 gives the spectrum of the stator current for a healthy operation under an SVU.

From that figure, it can be noticed that there is an increase in the amplitude of the harmonic 200 Hz compared to the healthy case. This increase is due to the unbalance of the supply voltage.

8. 1. 3. Motor Operation in the Presence of the ITSC Fault Figure 7 illustrates the stator current spectrum for a balanced supply and with an ITSC fault of 8.33 % (that is six turns in short-circuit).

In reference to Figure 5, the stator current spectrum presented in Figure 7 depicts an increase in the magnitude of the characteristic harmonics of ITSC fault *($3f_s$)*, which is of the order of 200 Hz.

8. 1. 4. Motor Operation in the Presence of the MSP Figure 8 shows the stator current spectrum in the presence of the effect of the MSP (Kgsat = 0.06) with a balanced supply voltage.

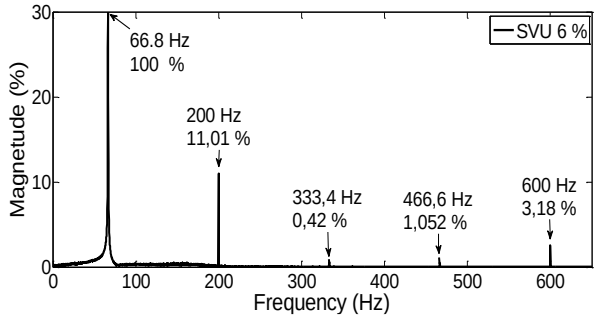

Figure 6. Healthy PMSM powered by an unbalanced voltage: Stator current spectrum

In the light of the results obtained, it is noticed that the frequencies due to the effect of the SVU are similar to the frequencies of the ITSC faults and that of the MSP.

According to these results, it is noted that the use of the technique of spectral analysis of the signature of the stator current is insufficient to discriminate between these three phenomena.

8. 2. Discrimination between ITSC Fault, MSP, and SVU Using the Proposed Approach The advantage of the proposed approach is the use not only of the amplitude but also the phase angle to discriminate between three phenomena (ITSC, MSP, and SVU).

The adaptation of the proposed algorithm is based on the amplitude and phase angle of the second harmonic obtained from the two indicators, voltage and current.

The results found are plotted in polar coordinates to simplify the interpretation and analysis of the different modes of operation.

8. 2. 1. Voltage Indicator Figure 9 shows the location of the harmonic reference *($2f_s$)* of the first indicator. This position represents the healthy operation of the motor (without faults) powered by a balanced voltage, and according to the figure, it is noted that the location of the plot is positioned in the first quadrant of the circle ($0 \leq \varphi \leq 90°$) in the polar coordinates graphical representation.

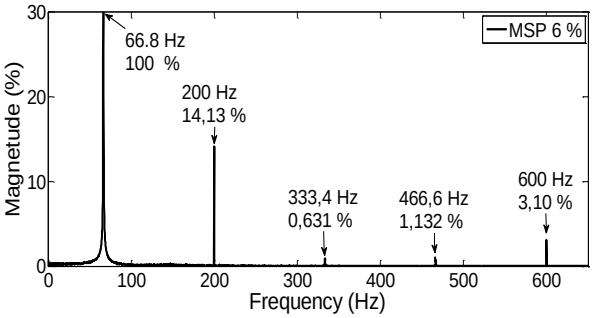

Figure 8. Motor operation in the presence of the MSP (Kgsat= 0.06): stator current spectrum

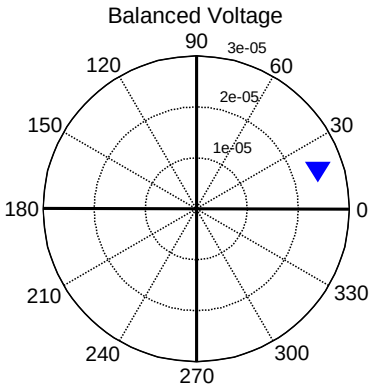

Figure 9. Position of the harmonic *(2f_s)* plot of the first indicator for the healthy operation a balanced voltage

On the one hand, if the healthy machine is powered by an unbalanced voltage source (Under-Voltage Unbalance UVU), this position occurs in the second quadrant of the circle around 120° (see Figure 10(a)). On the other hand, if the healthy machine is powered by an unbalanced voltage source (Over-Voltage Unbalance OVU), the position of the plot moves to the fourth quadrant of the circle around 300° (see Figure 10(b)). In the case of increasing the degree of the SVU (UVU), the plot position remains the same (in the same quadrant) but causes the displacement of the plot position upwards to the left from the center of the circle. In the same way, the increase of the SVU (OVU) degree does not modify the position of the plot, but only causes the displacement of the plot position down to the right.

8. 2. 2. Current indicator The location of the harmonic reference *(2f_s)* of the second indicator is illustrated in Figure 11. This position represents the healthy operation of the motor under a balanced power supply; this figure indicates that the location of the plot is at the first quadrant of the circle ($0 \leq \varphi \leq 90°$) in the graphical representation in polar coordinates.

The MSP is manifested by the plot position in the second quadrant of the circle around 120°, as shown in Figure 12. Moreover, increasing the saturation factor does not change the plot position, but causes the plot position to move upwards to the left from the center of the circle (Figure 12). In the case of an ITSC fault, the

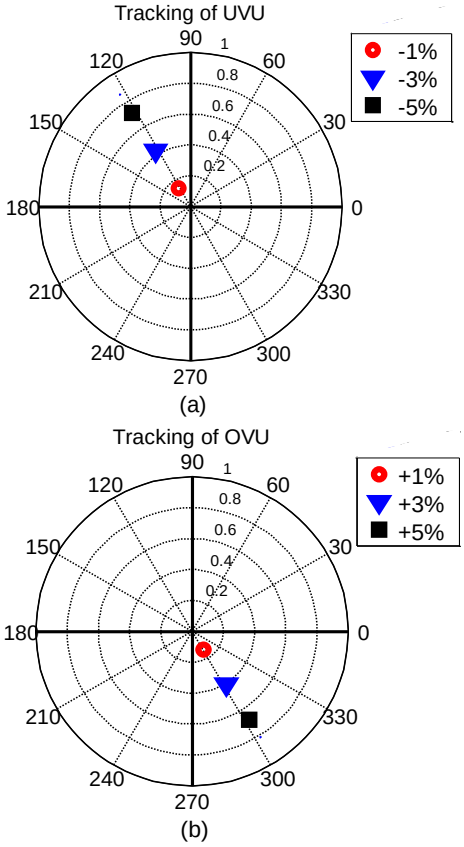

Figure 10. Position of the harmonic *(2f_s)* plot of the first indicator as a function of the severity of the SVU: (a) Under-voltage unbalance, (b) Over-voltage unbalance

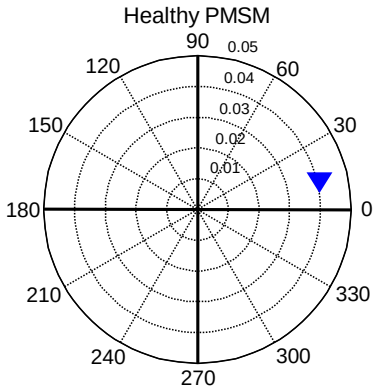

Figure 11. Position of the harmonic (*2f_s*) plot of the second indicator for the healthy PMSM under a balanced voltage

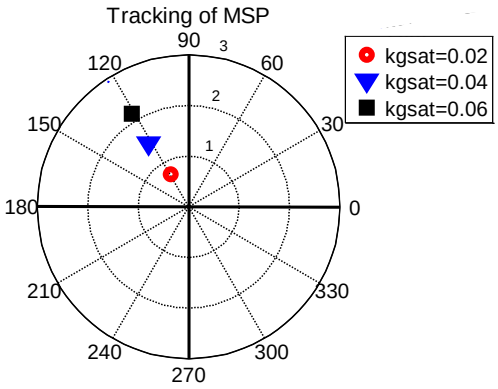

Figure 12. Position of the harmonic (*2f_s*) plot of the second indicator as a function of the severity of the MSP

plot is positioned in the third quadrant of the circle around 210° (Figure 13). Increasing the severity of the ITSC fault causes the position to move down to the left from the center of the circle in the same quadrant.

The simultaneous presence of the ITSC fault and the MSP is manifested by an intermediate position relative to the two phenomena (between the second and third quadrants), as shown in Figure 14. This position can vary between the second and third quadrant depending on the predominance of the phenomenon:

- In the second quadrant, if the MSP is predominant (see Figure 14 in blue).
- In the third quadrant, if the ITSC fault is predominant (see Figure 14 in black).

As indicated at the end of section 7, the presence of the SVU does not influence the current indicator, and the presence of the MSP or the ITSC fault does not influence the voltage indicator.

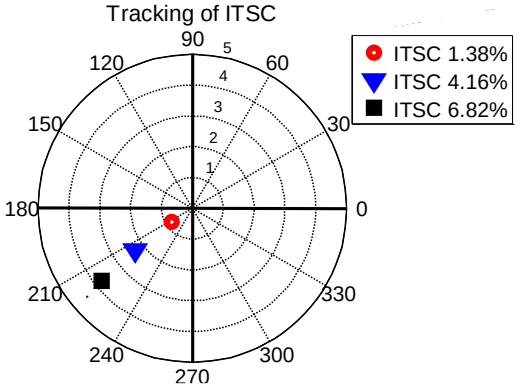

Figure 13. Position of the harmonic ($2f_s$) plot of the second indicator as a function of the severity of the ITSC Fault

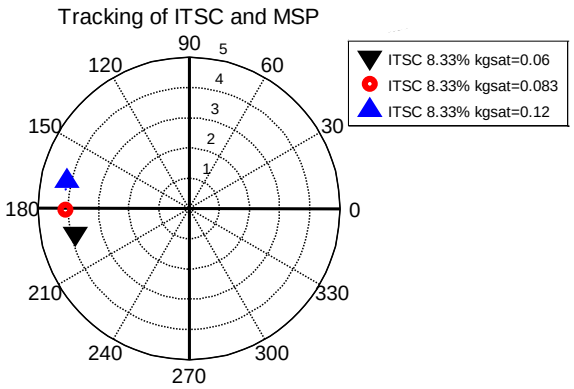

Figure 14. Position of the harmonic ($2f_s$) plot of the second indicator as a function of the severity of the ITSC Fault and the MSP

Therefore, to diagnose the ITSC fault in the presence of the SVU, it is sufficient to track the current and voltage indicator plot position simultaneously. Our study shows that if the PMSM experiences an ITSC fault and powered by an unbalanced voltage source (UVU), the voltage indicator plot position takes place in the second quadrant of the circle around 120° (see Figure 10(a)) and the current indicator plot position takes place in the third quadrant of the circle around 210° (Figure 13).

On the other hand, if the PMSM is powered by an unbalanced voltage source (OVU), the position of the voltage indicator plot moves to the fourth quadrant of the circle around 300° (see Figure 10(b)). Otherwise, the position of the current indicator plot always remains in the third quadrant (see Figure 13).

The different positions of the voltage and current indicators, depending on the state of the machine and the power source, are summarized in Table 1.

TABLE 1. Position of voltage and current indicators for different cases of operation

Plot Position	Healthy PMSM	SVU		ITSC	MSP	SVU and ITSC	
		UVU	OVU			UVU	OVU
Voltage Indicator	Q1	Q2	Q4	------	------	Q2	Q4
Current Indicator	Q1	------	------	Q3	Q2	Q3	Q3

9. CONCLUSION

In this paper, a new approach is proposed to discriminate between the inter-turns short-circuit fault, the magnetic saturation phenomenon, and the supply voltage unbalances in permanent magnets synchronous motors.

This approach is based on the tracking of the simultaneous position of the polar coordinates of the amplitude and phase angle of the signals of the voltage and current indicators of the harmonic characteristics of the three phenomena. These indicators are based on the supply voltages (Vsa, Vsb, and Vsc) and the stator currents (Isa, Isb, and Isc) that are available in any drive system and do not require additional hardware.

The simulation results prove the effectiveness and reliability of the proposed approach. For this purpose, the method using polar graphical representation shows better readability in terms of the spectrum and speed of decision making concerning the distinction between these three phenomena (ITSC, MSP, and the SVU).

10. REFERENCES

1. M'hamed, L., Zakaria, G. and Khireddine, D. "A Robust Sensorless Control of PMSM Based on Sliding Mode Observer and Model Reference Adaptive System." ***International Journal of Power Electronics and Drive System (IJPEDS)***, Vol. 8, No. 3, (2017), 1016–1025. https://doi.org/10.11591/ijpeds.v8i3.pp1016-1025
2. Faiz, J., and Hassan-Zadeh, M. R. "Impacts of eccentricity fault on permanent magnet generators for distributed generation." In Proceedings - 2017 International Conference on Optimization of Electrical and Electronic Equipment, OPTIM 2017 and 2017 Intl Aegean Conference on Electrical Machines and Power Electronics, ACEMP 2017, (2017), 434–441. https://doi.org/10.1109/OPTIM.2017.7975008
3. Arehpanahi, M., and Kheiry, E. "A New Optimization of Segmented Interior Permanent Magnet Synchronous Motor Based on Increasing Flux Weakening Range and Output Torque (Research Note)." ***International Journal of Engineering - Transactions C: Aspects***, Vol. 33, No. 6, (2020), 1122–1127. https://doi.org/10.5829/ije.2020.33.06c.09
4. Arish, N., and Teymoori, V. "Development of Linear Vernier Hybrid Permanent Magnet Machine for Wave Energy Converter." ***International Journal of Engineering - Transactions B: Applications***, Vol. 33, No. 5, (2020), 805–813. https://doi.org/10.5829/IJE. 2020.33.05B.12
5. Faiz, J., and Exiri, S. A. H. "Short-circuit fault diagnosis in permanent magnet synchronous motors- an overview." In ACEMP 2015: Aegean Conference on Electrical Machines and Power Electronics, OPTIM 2015: Optimization of Electrical and Electronic Equipment and ELECTROMOTION 2015: International Symposium on Advanced Electromechanical Motion Systems, (2015), 18–27. https://doi.org/10.1109/OPTIM.2015.7427038
6. Zafarani, M., Bostanci, E., Qi, Y., Goktas, T., and Akin, B. "Interturn short-circuit faults in permanent magnet synchronous machines: An extended review and comprehensive analysis." ***IEEE Journal of Emerging and Selected Topics in Power Electronics***. Vol. 6, No. 4, (2018), 2173-2191. https://doi.org/10.1109/JESTPE.2018.2811538
7. Qi, Y., Bostanci, E., Gurusamy, V., and Akin, B. "A Comprehensive Analysis of Short-Circuit Current Behavior in PMSM Interturn Short-Circuit Faults." ***IEEE Transactions on Power Electronics***, Vol. 33, No. 12, (2018), 10784–10793. https://doi.org/10.1109/tpel.2018.2809668
8. Haddad, R. Z., and Strangas, E. G. "On the Accuracy of Fault Detection and Separation in Permanent Magnet Synchronous Machines Using MCSA/MVSA and LDA." ***IEEE Transactions on Energy Conversion***. Vol. 31, No. 3, (2016), 924-934. https://doi.org/10.1109/TEC.2016.2558183
9. Çira, F., Arkan, M., and Gümüş, B. "A new approach to detect stator fault in permanent magnet synchronous motors." In Proceedings - SDEMPED 2015: IEEE 10th International Symposium on Diagnostics for Electrical Machines, Power Electronics and Drives, (2015), 316–321. https://doi.org/10.1109/DEMPED.2015.7303708
10. Li, H., Hang, J., Fang, J., Zhang, P., Ding, S., and Wang, Q. "Inter-turn fault diagnosis of permanent magnet synchronous machine based on variational mode decomposition." In Proceedings of the 13th IEEE Conference on Industrial Electronics and Applications, ICIEA 2018, (2018), 2422–2425. https://doi.org/10.1109/ICIEA.2018.8398115
11. Hang, J., Zhang, J., Cheng, M., and Huang, J. "Online Interturn Fault Diagnosis of Permanent Magnet Synchronous Machine Using Zero-Sequence Components." ***IEEE Transactions on Power Electronics***, Vol. 30, No. 12, (2015), 6731–6741. https://doi.org/10.1109/TPEL.2015.2388493
12. Jeong, H., Lee, H., and Kim, S. W. "Classification and Detection of Demagnetization and Inter-Turn Short Circuit Faults in IPMSMs by Using Convolutional Neural Networks." In 2018 IEEE Energy Conversion Congress and Exposition, ECCE 2018, (2018), 3249–3254. https://doi.org/10.1109/ECCE.2018.8558191
13. Li, X., Han, L., Xu, H., Yang, Y., and Xiao, H. "Rolling Bearing Fault Analysis by Interpolating Windowed DFT Algorithm." ***International Journal of Engineering - Transactions A: Basics***, Vol. 32, No. 1, (2018), 121–126. https://doi.org/10.5829/ije.2019.32.01a.16
14. Heidari, M. "Fault Detection of Bearings Using a Rule-based Classifier Ensemble and Genetic Algorithm." ***International Journal of Engineering - Transactions A: Basics***, Vol. 30, No. 4, (2017), 604–609. https://doi.org/10.5829/idosi.ije.2017.30.04a.20
15. Zaza, G., Hammou, A. D., Benchatti, A., and Saiah, H. "Fault Detection Method on a Compressor Rotor Using the Phase Variation of the Vibration Signal." ***International Journal of Engineering - Transactions B: Applications***, Vol. 30, No. 8, (2017), 1176–1181. https://doi.org/10.5829/ije.2017.30.08b.09
16. Eftekhari, M. "The Effect of Damping and Stiffness of Bearing on the Natural Frequencies of Rotor-bearing System." ***International Journal of Engineering - Transactions C: Aspects***, Vol. 30, No. 3, (2017), 448–455. https://doi.org/10.5829/idosi.ije.2017.30.03c.15
17. Refaat, S. S., Abu-Rub, H., Saad, M. S., Aboul-Zahab, E. M., and Iqbal, A. "Discrimination of stator winding turn fault and unbalanced supply voltage in permanent magnet synchronous motor using ANN." In International Conference on Power Engineering, Energy and Electrical Drives, (2013), 858–863. https://doi.org/10.1109/PowerEng.2013.6635722
18. Aberkane, M., Benouzza, N., Bendiabdellah, A., and Boudinar, A. H. "Discrimination between supply unbalance and stator short-circuit of an induction motor using neural network." ***International Review of Automatic Control***, Vol. 10, No. 5, (2017), 451–460. https://doi.org/10.15866/ireaco.v10i5.11912
19. Harir, M., Bendiabdellah, A., and Boudinar, A. H. "A proposed technique for discrimination between saturation phenomenon and short-circuit faults in induction motor." ***International Review on Modelling and Simulations***, Vol. 11, No. 5, (2018), 333–342. https://doi.org/10.15866/iremos.v11i5.15465
20. Zhang, C., Luo, L., He, J., and Liu, N. "Analysis of the short-circuit fault characteristics of permanent magnet synchronous machines." In Proceedings - 2015 Chinese Automation Congress, CAC 2015, (2015) 1913–1917. https://doi.org/10.1109/CAC.2015.7382816
21. Gherabi, Z., Toumi, D., Benouzza, N., and Henini, N. "Modeling and Diagnosis of Stator Winding Faults in PMSM using Motor Current Signature Analysis." In Proceedings 2019 International Aegean Conference on Electrical Machines and Power Electronics, ACEMP 2019 and 2019 International Conference on Optimization of Electrical and Electronic Equipment, OPTIM 2019, (2019), 227–232. https://doi.org/10.1109/ACEMP-OPTIM44294.2019.9007162
22. Lai, C., Aiswarya, B., Vicki, B., Lakshmi Varaha Iyer, K., and Kar, N. C. "Analysis of stator winding inter-turn short-circuit fault in interior and surface mounted permanent magnet traction machines." In 2014 IEEE Transportation Electrification Conference and Expo: Components, Systems, and Power Electronics - From Technology to Business and Public Policy, ITEC 2014, (2014), 1-6. https://doi.org/10.1109/itec.2014.6861775
23. Liang, W., Fei, W., and Luk, P. C. K. "An Improved Sideband Current Harmonic Model of Interior PMSM Drive by Considering Magnetic Saturation and Cross-Coupling Effects." ***IEEE Transactions on Industrial Electronics***, Vol. 63, No. 7, (2016), 4097–4104. https://doi.org/10.1109/TIE.2016.2540585

24. Nandi, S. “An Extended Model of Induction Machines with Saturation Suitable for Fault Analysis.” In Conference Record - IAS Annual Meeting (IEEE Industry Applications Society- Vol. 3), (2003), 1861–1868. https://doi.org/10.1109/ias.2003.1257822
25. Gherabi, Z., Djilali, T., Benouzza, N., and Denai, M. “Stator Inter-Turn Short-Circuit and Eccentricity Faults Detection in Permanent Magnet Synchronous Motors Using Line Current Spectrum Analysis.” ***International Review of Electrical Engineering***, Vol. 15, No. 1, (2020), 54–68. https://doi.org/10.15866/iree.v15i1.17638
26. Refaat, S. S., Abu-Rub, H., Mohamed, A., and Trabelsi, M. “Investigation into the effect of unbalanced supply voltage on detection of stator winding turn fault in PMSM.” In Proceedings of the IEEE International Conference on Industrial Technology, (2017), 312–317. https://doi.org/10.1109/ICIT.2017.7913102
27. Lee, C. Y. “Effects of unbalanced voltage on the operation performance of a three-phase induction motor.” ***IEEE Transactions on Energy Conversion***, Vol. 14, No. 2, (1999), 202–208. https://doi.org/10.1109/60.766984
28. Sahu, S., Dash, R. N., Panigrahi, C. K., and Subudhi, B. “Unbalanced voltage effects and its analysis on an induction motor.” In IEEE International Conference on Innovative Mechanisms for Industry Applications, ICIMIA 2017 - Proceedings, (2017), 263–268. https://doi.org/10.1109/ICIMIA.2017.7975616
29. Nandi, S., Toliyat, H. A., and Parlos, A. G. “Performance analysis of a single phase induction motor under eccentric conditions.” In Conference Record - IAS Annual Meeting (IEEE Industry Applications Society) (Vol. 1), (1997), 174–181. https://doi.org/10.1109/ias.1997.643024
30. Joksimović, G. M., Durović, M. D., Penman, J., and Arthur, N. “Dynamic simulation of dynamic eccentricity in induction machines - winding function approach.” ***IEEE Transactions on Energy Conversion***, Vol. 15, No. 2, (2000), 143–148. https://doi.org/10.1109/60.866991
31. Liang, Z., Liang, D., and Jia, S. “Inductance Calculation for the Symmetrical Non-Salient Dual Three-Phase PMSM Based on Winding Function Approach.” In ICEMS 2018 - 2018 21st International Conference on Electrical Machines and Systems, (2018), 269–274. https://doi.org/10.23919/ICEMS.2018.8549109
32. Gherabi, Z., Benouzza, N., Toumi, D., and Bendiabdellah, A. “Eccentricity Fault diagnosis in PMSM using Motor Current Signature Analysis.” In Proceedings 2019 International Aegean Conference on Electrical Machines and Power Electronics, ACEMP 2019 and 2019 International Conference on Optimization of Electrical and Electronic Equipment, OPTIM 2019, (2019), 205–210. https://doi.org/10.1109/ACEMP-OPTIM44294.2019.9007164

11. APPENDIX

TABLE A. PMSM parameters

Symbol	Description	Values	Units
V_n	Rated voltage	150	*V*
f_s	Rated frequency	66.7	*Hz*
I_n	Rated current	15.1	*A*
C_n	Rated torque	17.5	*Nm*
$\square_n$	Rated speed	2000	*rpm*
R_s	Stator resistance	0.295	Ω
L_s	Synchronous inductance	3.5	*mH*
J	Moment of inertia	3.10^{-4}	$Kg.m^2$
F	Viscous rubbing	0.017	*Nm/rad/s*
P	Number of pole pairs	2	-----
g_o	Nominal air gap	12	*mm*
r	Stator radius	64	*mm*
rr	Rotor radius	52	*mm*
l	Length of the machine	250	*mm*
N_s	Number of turn/coils	6	-----
h	Thickness of magnets	10	*mm*

Persian Abstract

چکیده

این مقاله یک رویکرد جدید از تبعیض بین گسل اتصال کوتاه، پدیده اشباع مغناطیسی (MSP) و عدم تعادل ولتاژ تأمین (SVU) در موتورهای همزمان آهن‌ربا (PMSMs) ارائه شده است. این رویکرد در پیگیری موقعیت همزمان در مختصات قطبی دامنه و زاویه فاز ولتاژ و سیگنال‌های FFT نشانگر جریان از همسازهای توصیف شده از سه پدیده است. نشانگر ولتاژ با استفاده از سه ولتاژ منبع تغذیه برای بررسی وضعیت منبع تغذیه تنظیم می‌شود. به همین روش، نشانگر جریان با استفاده از سه جریان خط برای تفکیک بین گسل ITSC و MSP تعریف می‌شود. برای برجسته کردن اثربخشی این رویکرد؛ یک سری شبیه‌سازی بر روی سیگنال‌های به دست آمده از یک مدل ریاضی از PMSM انجام می‌شود. این مدل در یک پسوند 2D از رویکرد عملکرد سیم پیچ اصلاح شده است.